axioms

MDPI

Article

Weighted-Likelihood-Ratio-Based EWMA Schemes for Monitoring Geometric Distributions

Yizhen Zhang [1], Hongxing Cai [2] and Jiujun Zhang [2,*]

[1] School of Mathematics and Statistics, Beihang University, Beijing 100191, China; 21377374@buaa.edu.cn
[2] School of Mathematics and Statistics, Liaoning University, Shenyang 110036, China; 17852032964@163.com
* Correspondence: zjjly790816@163.com

Abstract: Monitoring the parameter of discrete distributions is common in industrial production. Also, it is often crucial to monitor the parameter of geometric distribution, which is often regarded as the nonconforming item rate. To enhance the detection of nonconforming item, we designed an exponentially weighted moving average (EWMA) scheme based on the weighted likelihood ratio test (WLRT) method, and this scheme is denoted as the EWLRT scheme, specifically designed for monitoring the increase of the parameter in geometric distribution. Moreover, the optimal statistical design of the EWLRT scheme is presented when the shift is known. Results from numerical comparisons through Monte Carlo simulations indicates that the EWLRT scheme performs better than the competing schemes in some scenarios. Additionally, the designed scheme is characterized by its simplicity and ease of use, making it ideally suited for scenarios involving single observation. An example is illustrated to demonstrate the effectiveness of the EWLRT scheme.

Keywords: statistical process monitoring; process monitoring schemes; geometric distribution; weighted likelihood ratio test; exponentially weighted moving average

MSC: 62P30

check for updates

Citation: Zhang, Y.; Cai, H.; Zhang, J. Weighted-Likelihood-Ratio-Based EWMA Schemes for Monitoring Geometric Distributions. *Axioms* **2024**, *13*, 392. https://doi.org/10.3390/axioms13060392

Academic Editor: Hans J. Haubold

Received: 29 April 2024
Revised: 4 June 2024
Accepted: 7 June 2024
Published: 12 June 2024

Copyright: © 2024 by the authors. Licensee MDPI, Basel, Switzerland. This article is an open access article distributed under the terms and conditions of the Creative Commons Attribution (CC BY) license (https://creativecommons.org/licenses/by/4.0/).

1. Introduction

Statistical process monitoring (SPM) serves as the technical foundation for ensuring the stability of manufacturing processes and the quality of product outputs [1]. Process monitoring schemes are the most essential tools for monitoring the parameter of the discrete distributions within production processes. Since the seminal introduction of schemes by Shewhart, these tools have become fundamental in SPM, with widespread application across various industrial sectors [2]. These schemes are indispensable in the production line, particularly relevant to equipment maintenance, production decision-making, and pharmaceutical management [3]. Traditional monitoring schemes, such as the Shewhart scheme, are adept at identifying large process shifts, while cumulative sum (CUSUM) and exponentially weighted moving average (EWMA) schemes are effective for detecting small-to-moderate shifts.

Despite the proven effectiveness of traditional SPM schemes in various scenarios, these schemes are based on the presumption of a normal distribution that is not universally present in real-world settings, presenting a limitation [4]. In recent years, this acknowledgment has stimulated the advancement of non-parametric and distribution-specific SPM methodologies, designed to more closely align with the distributional attributes of actual data [5]. The geometric distribution is a vital discrete probability distribution that has wide applications in practice [6]. Quesenberry [7] used Q statistics to detect shifts in the parameter of geometric distribution. Yang et al. [8] investigated the sample size effect when the process parameter needs to be estimated for geometric distribution. Chan et al. [9] proposed the cumulative probability scheme when processes with low defect rates can not be satisfactorily monitored using the traditional p-scheme, np-scheme, c-scheme, or

u-scheme. Zhang et al. [10] addressed several theoretic issues related to the design of geometric schemes. Based on geometric distribution, Hong and Lee [11] investigated the performance of Bayes estimator and maximum likelihood estimation for the geometric scheme, and Kim and Lee [12] used the Bayes estimator to design a geometric scheme with bootstrap-based control limits. Moreover, Mohammadian et al. [13] utilized risk-adjusted schemes to monitor health-care systems. Researchers are conducting further exploration into monitoring the parameter of geometric distribution (see Quesenberry [14], Schwertman [15], Majeed et al. [16], KazemiNia [17], Shahzad et al. [18], Park et al. [19]).

Amid the growing complexity of production processes, the pursuit of monitoring scheme enhancements and innovations has caught the research community's attention [20]. Notably, Zou and Tsung [21] proposed a distribution-agnostic EWMA scheme based on the weighted likelihood ratio, which stands out due to its exceptional ability to monitor shifts across location, scale, and shape parameters. Moreover, Aslam et al. [22] introduced a hybrid EWMA-CUSUM scheme for Weibull distribution traits, demonstrating heightened sensitivity to small process shifts. The application scope of EWMA schemes has also been broadened in recent years to include non-parametric and multivariate process monitoring. For instance, Riaz et al. introduced a sensitive non-parametric EWMA scheme in 2015 and a non-parametric double EWMA scheme in 2016 for an improved monitoring of process location [23,24]. Xue et al. [25] designed a non-parametric adaptive EWMA scheme for monitoring multivariate time-between-events-and-amplitude data.

In parallel, recent academic research has generated numerous schemes based on the weighted likelihood ratio test (WLRT), aimed at improving the detection of small-to-moderate process shifts. Zhou et al. [26] unveiled a WLRT-based EWMA scheme for overseeing Poisson processes. Qi et al. [27,28] used the WLRT scheme to monitor generalized linear profiles and queuing systems. Zhang et al. [29] proposed a WLRT scheme for monitoring censored lifetime data, and Yu et al. [30] presented an enhanced weighted Poisson CUSUM scheme based on the WLRT to monitor an overdispersed counting process. Yao et al. [31] used the WLRT scheme for monitoring polynomial profiles. Moreover, Song et al. [32] further extended the WLRT framework to design a scheme for simultaneous mean and variance monitoring in normal distribution processes. This situation makes it possible to study EWMA schemes supported by WLRT for detecting changes in the geometric distribution parameter. WLRT-based schemes, distinguished by their simplicity and minimal parameter requirements beyond smoothing factors and control limits, are straightforward to design and implement. The WLRT methodology, known for its robustness in identifying a range of parameter shifts, excels in detecting upward shifts and is apt for scenarios involving single observation.

In the contemporary environment, market competition is becoming increasingly fierce, and customer demands are also rising. High-quality production is becoming more and more essential. Although companies have taken various measures to strengthen product quality management and improve production processes, which have significantly reduced the nonconforming rate of products and ensured their quality, the generation of nonconforming products is inevitable due to various reasons in actual production. Therefore, in the process of achieving a small nonconforming rate, how to apply more efficient and accurate process monitoring schemes to achieve real-time monitoring of product quality, reduce the nonconforming rate, ensure production stability, and maximize enterprise production profits has become an urgent issue for companies and researchers. Therefore, maximizing the control of the small nonconforming rate is of great significance.

However, to the best of our knowledge, there is no studies on refined EWMA schemes employing the WLRT (EWLRT) to monitor the small nonconforming rate in geometric distributions, and this paper will fill this gap. The rest of this paper is structured as follows: Section 2 illustrates an overview of some existing schemes. Section 3 delves into the characteristics of the EWLRT scheme, computing the corresponding values of average run length (ARL) for different parameter situations with the Monte Carlo simulation. Additionally, Section 3 also provides the optimal statistical design of the EWLRT scheme

and the control limits under different parameter settings when the size of the shift is known. The performance comparison with other competing schemes is presented in Section 4. An example is included in Section 5 for validating the utility of the new EWLRT scheme. Section 6 contains conclusions for this research.

2. An Overview of Some Existing Schemes

The number of the conforming items produced preceding the first nonconforming item is modeled to follow a geometric distribution with the parameter p, so p is the rate of the nonconforming item that remains constant across the production. In the in-control (IC) state, the parameter p is set to be a value of p_0, which is precisely estimated during Phase I. Our focus lies in Phase II, where schemes are deployed to identify any factors that may degrade process quality, consequently leading to an increase in the parameter p within the range of $(0 < p < 1)$.

Let the random variable X_t represent the count of conforming items preceding the first nonconforming item being produced, where t is the t-th sample, and each sample involves only one observation. X_t $(t = 1, 2, 3...)$ are independent of each other, and when the variables are not independent, some transformation techniques can be used to transform a geometrically distributed quality characteristic to independent normal statistics [33]. However, in this paper, we focus on the process observations being independent. Furthermore, we denote the variable X_t, which follows a geometric distribution with nonconforming item rate of p_0, as $X_t \sim Ge(p_0)$. The probability mass function (PMF) of X_t is expressed as follows:

$$P(X_t = x_t) = (1 - p_0)^{x_t - 1} p_0, \quad t = 1, 2, 3, \ldots,$$

Next, we will provide a concise overview of several existing process monitoring schemes for geometric distribution, which include three competing schemes, namely the EWMA, CUSUM, and GLR (generalized likelihood ratio) schemes. These three schemes will also be included in the performance comparisons discussed in Section 4.

2.1. The EWMA Scheme

For the random variables $X_t \sim Ge(p_0)$, the EWMA scheme employs the statistic Z_t defined as follows:

$$Z_t = (1 - \lambda) Z_{t-1} + \lambda X_t, \quad t = 1, 2, \ldots, \tag{1}$$

where Z_0 is the process mean, and λ is the smoothing parameter. For the geometric distribution, the scheme's upper control limit (UCL), central line (CL), and lower control limit (LCL) are given as follows:

$$UCL = CL + L\sqrt{\frac{\lambda}{2 - \lambda}(1 - p_0)\frac{1}{p_0^2}}, \tag{2}$$

$$CL = \frac{1}{p_0}, \tag{3}$$

$$LCL = CL - L\sqrt{\frac{\lambda}{2 - \lambda}(1 - p_0)\frac{1}{p_0^2}}, \tag{4}$$

where L is a constant determined by the pre-specified value of IC ARL (ARL_0). A deviation of Z_t beyond the specified limits indicates a potential process shift, necessitating further examination.

2.2. The CUSUM Scheme

For swifter detecting of small-to-moderate shifts in p, the CUSUM scheme represents a preferable alternative. By adjusting the preset out-of-control (OOC) nonconforming item rate p_a, where $p_a > p_0$, the scheme can enhance its sensitivity to variations close to p_a, and the efficiency of CUSUM in monitoring the parameter of geometric distribution highly

depends on the parameter of p_a. Suboptimal choices may result in inadequate detection capabilities for certain shifts. Thus, providing a rigorous framework for monitoring and acting upon incremental changes in process probabilities is necessary.

Under the assumption that when the process is IC up to the τ-th sample, then a change in p has occurred between samples τ and $\tau+1$, shifting to some OOC value. We are left with $X_1, X_2, \ldots, X_t$ after the t-th sample. Following the observation of t samples, we aim to assess if p has escalated from p_0 within the interval between τ and $\tau+1$ samples. The increment accumulated in the CUSUM statistic at sample i is given as follows:

$$\begin{aligned} \ln \frac{P(X_i|p_a)}{P(X_i|p_0)} &= \ln \frac{(1-p_a)^{X_i} p_a}{(1-p_0)^{X_i} p_0} \\ &= X_i \ln\left(\frac{1-p_a}{1-p_0}\right) + \ln\left(\frac{p_a}{p_0}\right) \end{aligned} \tag{5}$$

Then, the statistic of the CUSUM scheme is as follows:

$$\begin{aligned} C_t &= \max_{0\le\tau<t} \sum_{i=\tau+1}^{t} \left[X_i \ln\left(\frac{1-p_a}{1-p_0}\right) + \ln\left(\frac{p_a}{p_0}\right)\right] \\ &= \max\{0, C_{t-1}\} + X_t \ln\left(\frac{1-p_a}{1-p_0}\right) + \ln\left(\frac{p_a}{p_0}\right) \end{aligned} \tag{6}$$

The CUSUM scheme signals when $C_t > h_C$, where h_C is a predetermined control limit chosen to achieve the desired IC performance.

2.3. The GLR Scheme

GLR schemes break away from the fixed-parameter characteristic of CUSUM or EWMA schemes. GLR schemes excel in pinpointing process shifts, and this ability to monitor adaptive fluctuations emphasizes the exceptional versatility and adaptability of these schemes, making them well-suited for the dynamic and unpredictable characteristics of production environments.

The formula for the one-sided geometric distribution GLR statistic, aimed at detecting an increase in $p = p_1$, is shown as follows:

$$L(\tau, p_1|X_1, X_2, \ldots, X_t) = \prod_{i=1}^{\tau}(1-p_0)^{X_i} p_0 \times \prod_{i=\tau+1}^{t}(1-p_1)^{X_i} p_1, \tag{7}$$

$$\begin{aligned} R_t &= \ln \frac{\max_{0\le\tau<t, p_0\le p_1<1} L(\tau, p_1|X_1, X_2, \ldots, X_t)}{L(\infty, p_0|X_1, X_2, \ldots, X_t)} \\ &= \ln \frac{\max_{0\le\tau<t, p_0\le p_1<1} \prod_{i=\tau+1}^{t}(1-p_1)^{X_i} p_1}{\prod_{i=\tau+1}^{t}(1-p_0)^{X_i} p_0} \\ &= \max_{0\le\tau<t}\left[\sum_{i=\tau+1}^{t}\left(X_i \ln\frac{1-p_1}{1-p_0} + \ln\frac{p_1}{p_0}\right)\right], \end{aligned} \tag{8}$$

The maximum likelihood estimation of p_1 is given by the following:

$$\hat{p}_1 = \frac{t-\tau}{\sum_{i=\tau+1}^{t}(X_i+1)}, \tag{9}$$

Therefore, the statistic of the GLR scheme is reduced to the following:

$$R_t = \max_{0\le\tau<t}\left[\sum_{i=\tau+1}^{t}\left(X_i \ln\frac{1-\hat{p}_1}{1-p_0} + \ln\frac{\hat{p}_1}{p_0}\right)\right], \tag{10}$$

Maximizing over $0 \le \tau < t$ at each sampling point may be computationally complex when t is very large, so an alternative is to maximize only for a window of the past m

samples [34]. Let $R_{m,t}$ be the GLR scheme statistic when maximization is taken over $0 \leq \tau < t$ if $t \leq m$ and over $t - m \leq \tau < t$ if $t > m$. The window size m will be chosen to be large enough such that the performance of the GLR scheme with the window is essentially the same as that using no window. The GLR scheme for geometric distribution signals when $R_{m,t} > h_{GLR}$, where h_{GLR} is the predetermined control limit.

3. The EWLRT Scheme for Geometric Distribution

For the monitoring of the parameter for geometric distribution, schemes that utilize the likelihood ratio test have emerged as essential tools for monitoring the nonconforming item rate p. These schemes go beyond conventional likelihood ratio analysis, which traditionally depends on the current sample alone, by employing a weighted likelihood ratio method. This novel method enhances the monitoring effectiveness by assigning dynamic weights to the likelihood ratios of evolving samples, thereby leveraging the entirety of the sample data. The cumulative integration of historical data markedly bolsters the detection of shifts in the process parameter.

This paper unveils an extended EWMA scheme based on WLRT for detecting shifts in the geometric distribution parameter p. Through various performance evaluation metrics, this study appraised the effectiveness of this scheme in monitoring the parameter of geometric distribution. For simplicity, this new scheme is henceforth designated as the EWLRT scheme for geometric distribution.

3.1. Design of the EWLRT Scheme for Geometric Distribution

In order to maintain consistency with the notation previously defined, we still assume that each IC data X_i follows a geometric distribution with parameter $p = p_0$, where p_0 is known a priori, and this model transitions to $p = p_1$ when the process is OOC. The hypothesis test is formulated as follows:

$$H_0 : p = p_0 \quad \Longleftrightarrow \quad H_1 : p > p_0. \tag{11}$$

The log-likelihood function for a singular observation X_i is given by the following:

$$l_i(p) = l(p|X_i) = (X_i - 1)\ln(1 - p) + \ln p. \tag{12}$$

Assigning varying weights to samples as time progresses, we assume the following:

$$Y_t(p, \lambda) = \sum_{i=0}^{t} w_{i,\lambda} l_i(p), \tag{13}$$

with λ, the smoothing parameter, lying within (0 , 1]. Let $w_{i,\lambda}$ be the weights of EWMA, expressed as follows:

$$w_{i,\lambda} = \begin{cases} (1-\lambda)^t & \text{if } i = 0, \\ \lambda(1-\lambda)^{t-i} & \text{if } i \neq 0, \end{cases} \tag{14}$$

where $X_0 = \frac{1}{p_0}$ serves as an initial value. Given λ, the weighted maximum likelihood estimation for p is given by the following:

$$\hat{p} = \arg\max_{p} Y_t(p, \lambda). \tag{15}$$

The computation of Equation (13) unfolds as follows:

$$Y_t(p, \lambda) = \sum_{i=0}^{t} w_{i,\lambda}[(X_i - 1)\ln(1 - p) + \ln p] \tag{16}$$

$$= Y_{1,t}\ln(1 - p) + \ln p - \ln(1 - p), \tag{17}$$

where $Y_{1,t} = \sum_{i=0}^{t} w_{i,\lambda} X_i$. From the derivative $\frac{\partial Y_t(p,\lambda)}{\partial p} = 0$ and under the restriction $p > p_0$, it follows that

$$\hat{p} = \max\left\{\frac{1}{Y_{1,t}}, p_0\right\}, \tag{18}$$

Therefore, the EWLRT scheme's statistic is as follows:

$$R_{t,\lambda} = 2[Y_t(\hat{p},\lambda) - Y_t(p_0,\lambda)] \tag{19}$$

$$= 2Y_{1,t} \ln\frac{1-\hat{p}}{1-p_0} + 2\ln\frac{\hat{p}}{p_0} + 2\ln\frac{1-p_0}{1-\hat{p}}. \tag{20}$$

with the recursion applied to $Y_{1,t}$ as follows:

$$Y_{1,t} = (1-\lambda)Y_{1,t-1} + \lambda X_t, \tag{21}$$

initiating with $Y_{1,0} = \frac{1}{p_0}$. The monitoring of the parameter p utilizes the statistic $R_{t,\lambda}$ within the EWLRT scheme, integrating WLRT with EWMA for an optimized monitoring strategy.

Interestingly, with samples from a geometric distribution and as $\lambda t \to \infty$, $\lambda \to 0$, the following can be derived:

$$\frac{p_0^2}{(1-p_0)^2 \sum_{i=1}^{t} w_{i,\lambda}^2} R_{t,\lambda} \to \chi^2(1) \tag{22}$$

The proof of the asymptotic distribution (22) is given in the Appendix A, and this result indicates that, for substantial t, the asymptotic distribution's quantiles can serve as control limits. Moreover, we assume that the control limit for the EWLRT scheme is h, and an alarm signal will be generated when $R_{t,\lambda} > h$.

3.2. Performance Metric

In this study, Monte Carlo simulation techniques were leveraged to perform an extensive series of simulations aimed at determining control limits and ARL values. The methodology involved setting the number of experimental iterations to 10,000. The investigation primarily utilized the zero-state ARL (ZS-ARL) as a crucial metric for assessing the performance of schemes.

The calculation of the ZS-ARL involves assuming that a persistent shift in the parameter occurs at the start of Phase-II monitoring. Moreover, in this paper, ZS-ARL in its IC and OOC states is represented as ARL_0 and ARL_1, respectively. The ARL_0 metric is instrumental in evaluating the sensitivity of schemes to Type I error—instances where the scheme indicates an alarm despite the process operating in control. An elevated ARL_0 value is preferable, as it reduces the likelihood of false alarms attributed to IC process variation.

3.3. Control Limits

Table 1 presents the control limits of the EWLRT scheme for different combinations of p_0, λ, and ARL_0. When considering fixed combinations of (p_0, λ) values, the control limit h demonstrates an approximate linear relationship with the logarithm of the ARL_0. Therefore, linear interpolation can be employed to determine the corresponding h values for ARL_0 values that are not listed in Table 1. We illustrate the utilization of Table 1 to determine h for the EWLRT scheme through an example.

Table 1. Control limits of the EWLRT scheme.

		ARL_0				
p_0	λ	**200**	**300**	**350**	**400**	**500**
0.01	0.05	0.0860	0.1069	0.1156	0.1229	0.1347
	0.10	0.2290	0.2679	0.2846	0.2978	0.3198
	0.20	0.5610	0.6380	0.6647	0.6871	0.7277
	0.40	1.3440	1.4802	1.5370	1.5771	1.6583
0.02	0.05	0.0926	0.1151	0.1237	0.1312	0.1438
	0.10	0.2417	0.2855	0.3015	0.3142	0.3382
	0.20	0.5901	0.6675	0.6970	0.7217	0.7632
	0.40	1.4110	1.5570	1.6146	1.6640	1.7412
0.03	0.05	0.1004	0.1243	0.1334	0.1415	0.1543
	0.10	0.2563	0.3021	0.3185	0.3330	0.3546
	0.20	0.6180	0.7005	0.7300	0.7560	0.8030
	0.40	1.4812	1.6393	1.7020	1.7494	1.8324
0.05	0.05	0.1186	0.1434	0.1534	0.1630	0.1786
	0.10	0.2889	0.3368	0.3554	0.3722	0.3971
	0.20	0.6824	0.7722	0.8060	0.8336	0.8831
	0.40	1.6392	1.8173	1.8846	1.9476	2.0466

Suppose samples are taken every 8 h from a product manufacturing process (i.e., observing the number of conforming items before the first non-conforming item is produced), with the aim of having false alarms occur no more than once every 5 months on average. Assuming a month consists of 30 days, then 5 months correspond to $3 \times 30 \times 5 = 450$ samples (i.e., $ARL_0 = 450$). In this example, $p_0 = 0.01$ and $\lambda = 0.05$ are considered. Therefore, according to Table 1, we observe that the corresponding values of h are 0.1229 and 0.1347 for ARL_0 = 400 and 500, respectively. The linear interpolation used to determine h for achieving the desired ARL_0 = 450 is as follows:

$$h = 0.1229 + (0.1347 - 0.1229)\frac{\ln(450) - \ln(400)}{\ln(500) - \ln(400)} = 0.1291, \tag{23}$$

With h = 0.1291, the simulated actual ARL_0 is 451.95, which is a practical and accurate approximation.

3.4. The Implementation of the EWLRT Scheme

In Table 2, it is apparent that EWLRT schemes with smaller λ values are optimally suited for detecting smaller shifts in the process. Moreover, schemes with larger λ values present enhanced sensitivity to larger shifts. The standard deviation of run length (SDRL) values associated with the schemes are considerably high, particularly for small shifts, sometimes nearing the schemes' ARL values. Moreover, in this paper, $SDRL$ in its IC and OOC states is denoted as $SDRL_0$ and $SDRL_1$, respectively. For example, when $\lambda = 0.4$, $p_0 = 0.01$ and $p_1 = 0.012$, the corresponding values of ARL_1 and $SDRL_1$ for the EWLRT scheme, are 147.29 and 144.10, respectively. Nonetheless, with the increase in shift magnitude, the decrease in SDRL values occurs at a rate significantly more pronounced than that of ARL values.

3.5. ARL Optimization for the EWLRT Scheme

In scenarios involving process parameter shift, the impact of varying smoothing parameters λ on the performance of the EWLRT scheme is significant. Generally, a smaller ARL_1 indicates improved detection capability. It is possible to determine the optimal smoothing parameter λ that minimizes the ARL_1 in a specific parameter shift scenario. This process involves matching appropriate control limits h for each λ, forming parameter pairs, with a desired ARL_0 while the process is being monitored in IC state ($p = p_0$). In situations where the shift size of the parameter p is known, a pair of λ and h can be found such that ARL_1 is minimized, which constitutes the optimal selection. The EWLRT scheme

we adopt is based on this logic to determine the best combination of λ and h for any given parameter shifts.

Table 2. ARL and $SDRL$ values of the EWLRT scheme for $p_0 = 0.01$.

	$\lambda = 0.05$		$\lambda = 0.1$		$\lambda = 0.2$		$\lambda = 0.4$	
p_1	**ARL**	**SDRL**	**ARL**	**SDRL**	**ARL**	**SDRL**	**ARL**	**SDRL**
0.010	350.37	326.45	350.11	336.98	350.25	342.08	350.02	338.30
0.012	76.88	60.80	90.98	78.95	114.51	104.33	147.29	144.10
0.014	38.52	23.44	41.85	30.42	52.68	44.42	80.22	75.61
0.017	23.00	9.83	23.25	12.94	27.16	19.76	40.52	35.42
0.020	17.59	5.77	16.59	7.15	17.81	10.76	25.40	20.73
0.030	12.03	2.28	10.51	2.57	9.66	3.60	11.05	6.77
0.040	10.37	1.38	8.76	1.50	7.63	1.96	7.62	3.43
0.050	9.57	0.98	8.01	1.07	6.73	1.36	6.29	2.30
0.100	8.28	0.46	6.84	0.50	5.40	0.56	4.45	0.72

For a predetermined ARL_0 value, a range of the variable λ from 0.01 to 1, increasing by 0.01 each time, we search for the (λ, h) that significantly reduces ARL_1 under a given shift $p = p_1$. Once these parameters and shift magnitude are fixed, ARL values can be derived through simulation calculations. Therefore, the ideal pairing of (λ, h) i.e., (λ^*, h^*), can be found through the following expression:

$$(\lambda^*, h^*) = \underset{(\lambda,h)}{\operatorname{argmin}}\, ARL(p_0, p_1, \lambda, h)$$

subject to the condition

$$ARL(p_0, p_0, \lambda^*, h^*) = ARL_0.$$

Table 3 shows the optimal selection results. When the process is IC, with $p = p_0$, and the $ARL_0 = 350$, we select $p_0 \in \{0.01, 0.02, 0.03, 0.05\}$. When the shift p_1 is determined, the optimal combinations of (λ, h) are identified where ARL_1 is minimized. For example, when $p_0 = 0.01$ and $p_1 = 0.012$, the optimal combinations of (λ, h), i.e., $(\lambda^*, h^*) = (0.01, 0.0101)$, and the value of ARL_1 are 68.99.

Table 3. Optimal combinations of (λ, h) for the EWLRT scheme at $ARL_0 = 350$.

$p_0 = 0.01$	p_1	0.012	0.014	0.017	0.020	0.05
	λ^*	0.01	0.03	0.06	0.11	0.35
	h^*	0.0101	0.0562	0.1480	0.3209	1.3043
	ARL_1	68.99	37.66	22.91	16.74	6.22
$p_0 = 0.02$	p_1	0.022	0.024	0.027	0.030	0.060
	λ^*	0.01	0.01	0.02	0.07	0.23
	h^*	0.0110	0.0113	0.0339	0.1932	0.8261
	ARL_1	68.91	43.41	31.08	16.71	9.65
$p_0 = 0.03$	p_1	0.032	0.034	0.037	0.040	0.070
	λ^*	0.01	0.01	0.02	0.04	0.16
	h^*	0.0129	0.0130	0.0382	0.1005	0.5597
	ARL_1	158.69	99.66	62.97	45.95	13.04
$p_0 = 0.05$	p_1	0.052	0.054	0.057	0.060	0.090
	λ^*	0.01	0.01	0.02	0.02	0.10
	h^*	0.0180	0.0182	0.0480	0.0482	0.3558
	ARL_1	220.42	150.95	102.28	75.12	20.47

4. Performance Comparisons with Competing Schemes

Exploring scenarios with nonconforming item rate $p_0 = 0.01$ and $p_0 = 0.1$, we aim for ARL_0 approximately equal to 350. Shifted nonconforming item rates p_1 are selected

across a broad range—$p_1 = 0.012, 0.014, 0.017, 0.020, 0.030, 0.040, 0.050$—for the smaller p_0 and extending up to $p_1 = 0.12, 0.14, 0.17, 0.20, 0.30, 0.40, 0.50$ for the larger p_0. This Section evaluates the performance of various schemes by analyzing their ARL_1 values.

4.1. The Comparison of the EWLRT and EWMA Schemes

According to Table 4, the EWLRT and EWMA schemes show comparable performance across most evaluated scenarios. Notably, the EWLRT schemes demonstrate a marginal advantage under certain conditions, particularly when dealing with larger λ values and smaller shifts in the parameter. For example, when $p_0 = 0.1$, $\lambda = 0.5$, and $p_1 = 0.12$, the values of ARL_1 corresponding to the EWLRT scheme and the EWMA scheme are 154.13 and 161.29, respectively.

Table 4. The ARL values of the EWLRT and EWMA schemes for $p_0 = 0.01, 0.1$.

	$\lambda = 0.05$		$\lambda = 0.10$		$\lambda = 0.15$		$\lambda = 0.20$		$\lambda = 0.50$	
p_1	EWLRT	EWMA	EWLRT	EWMA	EWLRT	EWMA	EWLRT	EWMA	EWLRT	EWMA
0.010	350.17	350.32	350.24	350.40	350.02	350.53	350.34	350.82	350.27	350.30
0.012	77.83	76.35	90.31	90.16	102.91	103.35	111.07	114.46	162.45	163.39
0.014	38.48	38.24	42.99	42.39	48.15	48.34	53.96	54.94	91.55	94.00
0.017	23.16	22.85	23.27	23.33	24.88	25.23	26.96	27.27	49.17	51.48
0.020	17.73	17.77	16.81	16.87	17.06	17.06	18.13	18.18	31.43	31.35
0.030	12.08	12.04	10.55	10.56	9.91	9.97	9.69	9.78	12.78	13.00
0.040	10.41	10.40	8.82	8.81	8.05	8.08	7.65	7.68	8.48	8.37
0.050	9.60	9.63	8.01	8.05	7.22	7.27	6.76	6.75	6.56	6.57
	$\lambda = 0.05$		$\lambda = 0.10$		$\lambda = 0.15$		$\lambda = 0.20$		$\lambda = 0.50$	
p_1	EWLRT	EWMA	EWLRT	EWMA	EWLRT	EWMA	EWLRT	EWMA	EWLRT	EWMA
0.10	350.29	350.29	350.84	350.32	350.01	350.08	350.34	350.15	350.20	350.71
0.12	78.00	77.85	87.77	88.67	96.89	98.37	108.29	110.58	154.13	161.29
0.14	40.22	40.37	41.57	41.94	46.21	46.44	51.40	51.66	85.84	89.35
0.17	25.09	24.98	23.01	23.10	23.56	23.73	25.45	25.73	45.05	44.83
0.20	19.49	19.55	16.86	17.00	16.52	16.56	16.87	17.06	27.71	27.61
0.30	13.73	13.68	10.94	10.96	9.82	9.87	9.33	9.33	11.13	11.02
0.40	11.92	11.90	9.25	9.27	8.12	8.12	7.45	7.47	7.35	7.18
0.50	11.07	11.07	8.49	8.48	7.35	7.31	6.65	6.66	5.77	5.67

Furthermore, the methodology for setting control limits distinguishes the two scheme types. EWLRT schemes utilize weighted likelihood ratio statistics to determine control limits, typically yielding smaller limit values. This characteristic of EWLRT schemes contributes to their stable performance amid small changes in p_0. Conversely, EWMA schemes base control limits on expected values, which can result in larger limit values and more pronounced performance fluctuations due to small changes in p_0, a trait less suited for practical manufacturing processes.

In practical production environments, the exact value of p_0 is often unknown ahead of time; instead, we depend on an estimation of p_0. Consequently, the effectiveness of the schemes should not be significantly affected by small adjustments in p_0. This subsection is dedicated to assessing the robustness of schemes by implementing a small shift to p_0 and then comparing the performance (measured in ARL_0) with the original p_0. In this paper, the original p_0 is the estimation of IC p from Phase I. A scheme is deemed robust if such alterations do not significantly impact its performance. Given the already-investigated ARL_1, with similar performance of the EWLRT and EWMA schemes in many cases, this analysis will focus on comparing the robustness between the EWLRT and EWMA schemes. The superior robustness of EWLRT schemes in comparison to EWMA schemes is shown in Table 5.

Table 5 illustrates that for the original nonconforming item rate of $p_0 = 0.01$, slight variations with the actual p_0 barely affect the ARL_0 values of the EWLRT scheme, dis-

tinguishing it significantly from the EWMA scheme where ARL_0 values are markedly influenced. For example, when the original p_0 is 0.01, the ARL_0 values for the EWLRT and EWMA schemes are both approximately 350, but when the actual p_0 is 0.008, the corresponding ARL_0 values for the EWLRT and EWMA schemes are 361.35 and 6531.7. For a larger original $p_0 = 0.1$, although small variations with the actual p_0 also impact the ARL_0 values of the EWLRT scheme, the degree of this impact is significantly less than that observed in the EWMA scheme.

These findings highlight the robustness of the EWLRT scheme, confirming its superiority over the EWMA scheme, particularly for geometric distributions characterized by smaller p_0 values. This analysis points out the EWLRT scheme as a more robust option and better suited for scenarios where p_0 is estimated rather than precisely known.

Table 5. The ARL_0 values of the EWLRT and EWMA schemes.

$\lambda = 0.05$	$p_0 = 0.01$ (Original1)	$p_0 = 0.008$	$p_0 = 0.009$	$p_0 = 0.011$	$p_0 = 0.012$
EWLRT	350.64	361.35	355.77	345.11	339.30
EWMA	350.99	6531.7	1429.4	129.97	56.24
$\lambda = 0.05$	$p_0 = 0.1$ (Original2)	$p_0 = 0.08$	$p_0 = 0.09$	$p_0 = 0.11$	$p_0 = 0.12$
EWLRT	350.58	506.59	417.98	298.42	255.71
EWMA	350.5	7848.7	2063.1	135.41	64.95
$\lambda = 0.10$	$p_0 = 0.01$ (Original1)	$p_0 = 0.008$	$p_0 = 0.009$	$p_0 = 0.011$	$p_0 = 0.012$
EWLRT	350.25	356.33	352.83	344.17	338.94
EWMA	340.41	4917.8	1390.7	156.64	81.03
$\lambda = 0.10$	$p_0 = 0.1$ (Original2)	$p_0 = 0.08$	$p_0 = 0.09$	$p_0 = 0.11$	$p_0 = 0.12$
EWLRT	350.56	504.09	418.31	297.92	251.73
EWMA	350.86	5091.9	1431.4	157.95	83.07
$\lambda = 0.15$	$p_0 = 0.01$ (Original1)	$p_0 = 0.008$	$p_0 = 0.009$	$p_0 = 0.011$	$p_0 = 0.012$
EWLRT	350.94	356.79	356.57	343.87	336.58
EWMA	350.64	3539.8	1179.6	173.55	99.25
$\lambda = 0.15$	$p_0 = 0.1$ (Original2)	$p_0 = 0.08$	$p_0 = 0.09$	$p_0 = 0.11$	$p_0 = 0.12$
EWLRT	350.33	514.04	422.64	298.28	246.21
EWMA	350.66	3694.6	1185.9	167.49	95.17
$\lambda = 0.20$	$p_0 = 0.01$ (Original1)	$p_0 = 0.008$	$p_0 = 0.009$	$p_0 = 0.011$	$p_0 = 0.012$
EWLRT	350.15	356.28	358.93	344.73	340.017
EWMA	350.36	2609.2	994.35	180.96	110.13
$\lambda = 0.20$	$p_0 = 0.1$ (Original2)	$p_0 = 0.08$	$p_0 = 0.09$	$p_0 = 0.11$	$p_0 = 0.12$
EWLRT	350.40	534.29	425.38	292.77	243.97
EWMA	350.37	2164.2	788.64	184.20	108.46
$\lambda = 0.50$	$p_0 = 0.01$ (Original1)	$p_0 = 0.008$	$p_0 = 0.009$	$p_0 = 0.011$	$p_0 = 0.012$
EWLRT	350.88	367.81	366.49	339.75	330.38
EWMA	350.42	1302.2	735.64	240.21	167.79
$\lambda = 0.50$	$p_0 = 0.1$ (Original2)	$p_0 = 0.08$	$p_0 = 0.09$	$p_0 = 0.11$	$p_0 = 0.12$
EWLRT	350.65	714.53	493.56	260.43	194.93
EWMA	350.55	1341.4	743.38	232.13	161.50

4.2. The Comparison of the EWLRT and CUSUM Schemes

Considering the different parameters of the EWLRT and CUSUM schemes, this subsection outlines the comparison of the optimal detection performance of the two schemes for specific shifts. The comparative result presented in Table 6 highlights the distinct advantages of EWLRT schemes over CUSUM schemes when monitoring small shifts, but

for large shifts, both schemes have a similar monitoring performance. For example, when $p_1 = 0.012$, the optimal parameters for the EWLRT scheme and the CUSUM scheme are 0.01 and 0.012, respectively, with corresponding ARL_1 values of 68.99 and 83.97. When $p_1 = 0.04$, the optimal parameters for the EWLRT scheme and the CUSUM scheme are 0.34 and 0.04, respectively, with corresponding ARL_1 values of 7.24 and 7.33.

Table 6. The ARL_1 values of the EWLRT and CUSUM schemes for $p_0 = 0.01, 0.1$.

$p_0 = 0.01$		EWLRT			CUSUM	
p_1	λ	h	ARL_1	p_a	h_C	ARL_1
0.012	0.01	0.0101	68.99	0.012	2.0201	83.97
0.014	0.03	0.0562	37.66	0.015	3.0995	44.63
0.017	0.06	0.1480	22.91	0.018	3.5985	25.77
0.020	0.11	0.3209	16.42	0.020	3.8014	18.15
0.030	0.24	0.8278	9.11	0.030	4.3000	9.96
0.040	0.34	1.2550	7.24	0.040	4.5003	7.33
0.050	0.35	1.3043	6.22	0.052	4.5987	6.24
$p_0 = 0.10$		EWLRT			CUSUM	
p_1	λ	h	ARL_1	p_a	h_C	ARL_1
0.12	0.03	0.1220	78.45	0.12	2.1005	81.12
0.14	0.06	0.2651	39.85	0.13	2.5899	42.41
0.17	0.12	0.5770	23.15	0.17	3.6017	23.77
0.20	0.14	0.6843	16.35	0.19	3.7972	16.61
0.30	0.27	1.4950	9.12	0.30	4.4003	8.84
0.40	0.38	2.3902	6.71	0.39	4.5005	6.34
0.50	0.44	3.0191	5.55	0.49	4.7012	5.51

4.3. The Comparison of the EWLRT and GLR Schemes

In this subsection, we outline the comparison of the performance of the EWLRT and GLR schemes for monitoring the geometric distribution parameter. When $ARL_0 = 350$, through simulation studies, it was found that the monitoring performance of the GLR scheme is similar when the window sizes $m = 100$ and $m = 200$ are chosen. Therefore, it is reasonable to select a window size of $m = 100$ when exploring the monitoring capability of the GLR scheme.

The comparison result, as detailed in Table 7, suggests that both the EWLRT and GLR schemes possess specific benefits. EWLRT schemes are particularly sensitive to small process shifts, whereas GLR schemes excel in detecting large shifts. For example, when $p_0 = 0.01$, $p_1 = 0.012$, and $\lambda = 0.05$, the values of ARL_1 corresponding to the EWLRT scheme and the GLR scheme are 78.83 and 131.74, respectively; meanwhile, when $p_1 = 0.04$, the values of ARL_1 corresponding to the EWLRT scheme and the GLR scheme are 10.41 and 7.31, respectively.

Table 7. The ARL values of the EWLRT and GLR schemes for $p_0 = 0.01, 0.1$.

			EWLRT			GLR
p_1	$\lambda = 0.05$	$\lambda = 0.10$	$\lambda = 0.15$	$\lambda = 0.20$	$\lambda = 0.50$	m = 100
0.010	350.17	350.24	350.02	350.34	350.27	350.23
0.012	78.83	90.31	102.91	111.07	162.45	131.74
0.014	38.48	42.99	48.15	53.96	91.55	59.67
0.017	23.16	23.27	24.88	26.96	49.17	29.75
0.020	17.73	16.81	17.06	18.13	31.43	19.74
0.030	12.08	10.55	9.91	9.69	12.78	9.99
0.040	10.41	8.82	8.05	7.65	8.48	7.31
0.050	9.60	8.01	7.22	6.76	6.56	6.02

Table 7. *Cont.*

	EWLRT					GLR
p_1	$\lambda = 0.05$	$\lambda = 0.10$	$\lambda = 0.15$	$\lambda = 0.20$	$\lambda = 0.50$	m = 100
0.10	350.29	350.84	350.01	350.34	350.20	350.91
0.12	78.00	87.77	96.89	108.29	154.13	115.44
0.14	40.22	41.57	46.21	51.40	85.84	50.51
0.17	25.09	23.01	23.56	25.45	45.05	25.26
0.20	19.49	16.86	16.52	16.87	27.71	16.76
0.30	13.73	10.94	9.82	9.33	11.13	8.43
0.40	11.92	9.25	8.12	7.45	7.35	5.93
0.50	11.07	8.49	7.35	6.65	5.77	4.82

The selection between EWLRT and GLR schemes should be customized based on the specific monitoring needs and process characteristics in the industry. A notable advantage of GLR schemes is their convenience in not necessitating a predefined parameter value, but they require a large amount of computation.

5. An Illustrative Example

To demonstrate the application of the EWLRT scheme, we use the dataset obtained from the CDR-Call Details Record, which can be downloaded from the following URL: https://www.kaggle.com/datasets/anshulmehtakaggl/cdrcall-details-record-predict-telco-churn (accessed on 4 June 2024). This is a call details dataset for studying customer satisfaction or predicting telecommunication churn. The telecom company calls customers in sequence based on their phone numbers to inquire about their satisfaction with the company's business and services, resulting in two outcomes: satisfied or dissatisfied—in other words, churned or non-churned customers. We consider the number of non-churned customers between two churned customers as a variable. A smaller value of this variable indicates a larger customer churn rate. Based on this, we can utilize the EWLRT scheme to monitor the customer churn rate.

Therefore, we can use the CDR-Call Details Record dataset to estimate the IC customer churn rate $\hat{p}_0$, obtaining $\hat{p}_0 = 0.1316$. The 40 samples in Table 8 represent the simulated shifted data, with a shift of $p_1 = 0.1974$. We choose $\lambda = 0.05, 0.1$ as the smoothing parameters of the EWLRT scheme, and the monitoring performance of the EWLRT scheme is shown in Figure 1. From Figure 1, the solid red line and the black dashed line, both with a slope of 0, represent the control limit of the EWLRT schemes with $\lambda = 0.05$ and $\lambda = 0.1$, respectively. We can observe that the EWLRT scheme generates a signal at the 24th sample with $\lambda = 0.05$ and at the 35th sample with $\lambda = 0.1$.

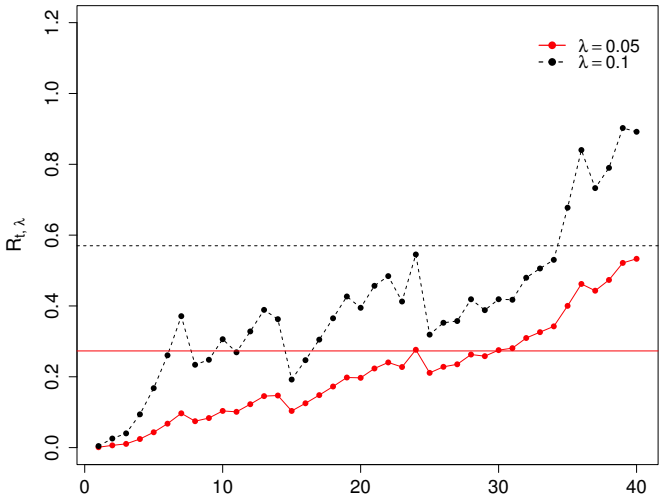


Figure 1. The performance of the EWLRT scheme for the illustrative example.

Table 8. The data for the illustrative example.

Churned Customer	Number of Non-Churned Customers	Churned Customer	Number of Non-Churned Customers
1	3	21	2
2	1	22	3
3	4	23	6
4	0	24	0
5	0	25	11
6	0	26	3
7	0	27	4
8	10	28	2
9	4	29	5
10	2	30	3
11	6	31	4
12	2	32	2
13	2	33	3
14	5	34	3
15	12	35	0
16	2	36	0
17	2	37	5
18	2	38	2
19	2	39	1
20	5	40	3

6. Conclusions

This paper analyzes and evaluates the EWLRT scheme that leverages the WLRT for monitoring changes in the parameter of geometric distribution within production processes. First, some existing schemes such as the EWMA, CUSUM, and GLR schemes for monitoring the parameter of geometric distribution are discussed. Then, the statistical properties of the EWLRT scheme are examined, and Monte Carlo simulations of this scheme are described. As anticipated, for the EWLRT scheme, larger parameters are more suitable for detecting large shifts, while smaller parameters are more suitable for detecting small shifts. In addition, we also investigated the control limits of the EWLRT scheme under different parameters and different ARL_0 values and provide a linear interpolation method for calculating these control limits after given ARL_0 values. Furthermore, the optimal EWLRT scheme is provided when the shift size is known. Through comprehensive simulation studies, it has been established that the EWLRT scheme distinctly outperforms conventional geometric distribution schemes in many cases in monitoring the parameter within production environments. Finally, the EWLRT scheme was applied to datasets related to customer churn rate, demonstrating different monitoring effects under different parameters.

Author Contributions: Conceptualization, Y.Z. and H.C.; methodology, Y.Z., H.C. and J.Z.; software, Y.Z. and H.C.; validation, Y.Z.; formal analysis, Y.Z.; investigation, Y.Z.; resources, Y.Z.; data curation, Y.Z. and H.C.; writing—original draft, Y.Z. and H.C.; writing—review & editing, Y.Z. and J.Z.; visualization, Y.Z.; supervision, Y.Z. and J.Z.; project administration, Y.Z. and J.Z. All authors have read and agreed to the published version of the manuscript.

Funding: This research was funded by the Project of the Education Department of Liaoning Province [grant number JYTMS20230768], the Research on Humanities and Social Sciences of the Ministry of Education [grant number 22YJC910009], the Doctoral Research Start-up Fund of Liaoning Province [grant number 2021-BS-142], the Education Department of Liaoning Province [grant number LJKZ1161, JYTMS20230767], the Natural Science Found of Anshan Normal University [grant number 23kyxm029].

Data Availability Statement: All data are available in the paper.

Conflicts of Interest: The authors declare no conflicts of interest.

Appendix A

Proof. Consider the statistic $R_{t,\lambda}$ defined as

$$R_{t,\lambda} = 2(Y_{1,t} \ln \frac{1-\hat{p}}{1-p_0} - \ln \frac{1-\hat{p}}{1-p_0} + \ln \frac{\hat{p}}{p_0}) \tag{A1}$$

Let $Q = \frac{p_0}{\hat{p}} = p_0 Y_{1,t}$. Under the null hypothesis H_0,

$$E(Q) = Q_0 = 1, \quad \text{Var}(Q) = (1-p_0) \sum_{i=1}^{t} w_{i,\lambda}^2 \tag{A2}$$

Define $Z = \frac{1}{\hat{p}} - Q$; hence $Z_0 = \frac{1}{\hat{p}} - 1$, and it follows that

$$E(Z) = \frac{1}{p_0} - 1, \quad \text{Var}(Z) = \frac{(1-p_0)^3}{p_0^2} \sum_{i=1}^{t} w_{i,\lambda}^2, \quad Z - Z_0 = Q_0 - Q \tag{A3}$$

Substituting Q and Z into $R_{t,\lambda}$ yields

$$R_{t,\lambda} = \frac{2}{\hat{p}}[\ln(\frac{1}{\hat{p}} - 1) - \ln(\frac{1}{\hat{p}} - Q)] - 2\ln(\frac{1}{\hat{p}} - 1) + 2\ln(\frac{1}{\hat{p}} - Q) - 2\ln Q \tag{A4}$$

$$= 2\left[\frac{1}{\hat{p}}(\ln Z_0 - \ln Z) - \ln Z_0 + \ln Z - \ln Q\right] \tag{A5}$$

$$= 2\left[(\frac{1}{\hat{p}} - 1)(\ln Z_0 - \ln Z) - \ln Q\right] \tag{A6}$$

$$= 2[Z_0(\ln Z_0 - \ln Z) - \ln Q] \tag{A7}$$

Employing Taylor's expansion, we have

$$\ln Z - \ln Z_0 = \frac{1}{Z_0}(Z - Z_0) - \frac{1}{2Z_0^2}(Z - Z_0)^2 + o((Z - Z_0)^2) \tag{A8}$$

$$\ln Q = \ln Q_0 + \frac{1}{Q_0}(Q - Q_0) - \frac{1}{2Q_0^2}(Q - Q_0)^2 + o((Q - Q_0)^2) \tag{A9}$$

$$= (Q - Q_0) - (Q - Q_0)^2 + o((Q - Q_0)^2) \tag{A10}$$

Therefore,

$$R_{t,\lambda} \approx -2\left[(Z - Z_0) - \frac{1}{2Z_0}(Z - Z_0)^2 + (Q - Q_0) - (Q - Q_0)^2\right] \tag{A11}$$

$$\approx \frac{1}{Z_0}(Z - Z_0)^2 + (Z - Z_0)^2 \tag{A12}$$

$$\approx \frac{1}{1-\hat{p}}(Z - Z_0)^2 \tag{A13}$$

$$\approx \frac{1}{1-\hat{p}} \frac{(1-p_0)^3}{p_0^2} \sum_{i=1}^{t} w_{i,\lambda}^2 \left(\frac{Z - Z_0}{\sqrt{\text{Var}(Z)}}\right)^2 \to \chi^2(1) \left(\frac{(1-p_0)^2}{p_0^2} \sum_{i=1}^{t} w_{i,\lambda}^2\right) \tag{A14}$$

Thus, we conclude that

$$\frac{p_0^2}{(1-p_0)^2 \sum_{i=1}^{t} w_{i,\lambda}^2} R_{t,\lambda} \to \chi^2(1) \tag{A15}$$

□

References

1. Joe Qin, S. Statistical process monitoring: Basics and beyond. *J. Chemom. A J. Chemom. Soc.* **2003**, *17*, 480–502. [CrossRef]
2. Zhao, C.; Lv, J.; Du, S. Geometrical deviation modeling and monitoring of 3D surface based on multi-output Gaussian process. *Measurement* **2022**, *199*, 111569. [CrossRef]
3. Zhou, Y.; Du, S.; Liu, M.; Shen, X. Machine-fixture-pallet resources constrained flexible job shop scheduling considering loading and unloading times under pallet automation system. *J. Manuf. Syst.* **2024**, *73*, 143–158. [CrossRef]
4. Zhao, C.; Du, S.; Deng, Y.; Li, G.; Huang, D. Circular and cylindrical profile monitoring considering spatial correlations. *J. Manuf. Syst.* **2020**, *54*, 35–49. [CrossRef]
5. Zhao, C.; Du, S.; Lv, J.; Deng, Y.; Li, G. A novel parallel classification network for classifying three-dimensional surface with point cloud data. *J. Intell. Manuf.* **2023**, *34*, 515–527. [CrossRef]
6. Kaminsky, F.C.; Benneyan, J.C.; Davis, R.D.; Burke, R.J. Statistical control charts based on a geometric distribution. *J. Qual. Technol.* **1992**, *24*, 63–69. [CrossRef]
7. Quesenberry, C.P. Geometric Q charts for high quality processes. *J. Qual. Technol.* **1995**, *27*, 304–315. [CrossRef]
8. Yang, Z.; Xie, M.; Kuralmani, V.; Tsui, K.L. On the performance of geometric charts with estimated control limits. *J. Qual. Technol.* **2002**, *34*, 448–458. [CrossRef]
9. Chan, L.Y.; Lin, D.K.; Xie, M.; Goh, T.N. Cumulative probability control charts for geometric and exponential process characteristics. *Int. J. Prod. Res.* **2002**, *40*, 133–150. [CrossRef]
10. Zhang, L.; Govindaraju, K.; Bebbington, M.; Lai, C.D. On the statistical design of geometric control charts. *Qual. Technol. Quant. Manag.* **2004**, *1*, 233–243. [CrossRef]
11. Hong, H.; Lee, J. Comparisons of the performance with Bayes estimator and MLE for control charts based on geometric distribution. *Korean J. Appl. Stat.* **2015**, *28*, 907–920. [CrossRef]
12. Kim, M.; Lee, J. Geometric charts with bootstrap-based control limits using the Bayes estimator. *Commun. Stat. Appl. Methods* **2020**, *27*, 65–77. [CrossRef]
13. Mohammadian, F.; Niaki, S.T.A.; Amiri, A. Phase-I risk-adjusted geometric control charts to monitor health-care systems. *Qual. Reliab. Eng. Int.* **2016**, *32*, 19–28. [CrossRef]
14. Quesenberry, C.P. Statistical process control geometric Q-chart for nosocomial infection surveillance. *Am. J. Infect. Control* **2000**, *28*, 314–320. [CrossRef] [PubMed]
15. Schwertman, N.C. Designing accurate control charts based on the geometric and negative binomial distributions. *Qual. Reliab. Eng. Int.* **2005**, *21*, 743–756. [CrossRef]
16. Majeed, M.Y.; Aslam, M.; Riaz, M. Mixture cumulative count control chart for mixture geometric process characteristics. *Qual. Quant.* **2013**, *47*, 2289–2307. [CrossRef]
17. KazemiNia, A.; Gildeh, B.S.; Abbasi Ganji, Z. The design of geometric generalized likelihood ratio control chart. *Qual. Reliab. Eng. Int.* **2018**, *34*, 953–965. [CrossRef]
18. Shahzad, F.; Huang, Z.; Shafqat, A. The design of GLR control chart for monitoring the geometric observations using sequential sampling scheme. *Symmetry* **2020**, *12*, 1964. [CrossRef]
19. Park, C.; Ouyang, L.; Wang, M. A study on the performance of the probability-limit control charts based on the geometric and negative binomial distributions. *Comput. Ind. Eng.* **2023**, *180*, 109275. [CrossRef]
20. Zhao, C.; Lui, C.F.; Du, S.; Wang, D.; Shao, Y. An earth mover's distance based multivariate generalized likelihood ratio control chart for effective monitoring of 3D point cloud surface. *Comput. Ind. Eng.* **2023**, *175*, 108911. [CrossRef]
21. Zou, C.; Tsung, F. Likelihood Ratio-Based Distribution-Free EWMA Control Charts. *J. Qual. Technol.* **2010**, *42*, 174–196. [CrossRef]
22. Aslam, M. A Mixed EWMA–CUSUM Control Chart for Weibull-Distributed Quality Characteristics. *Qual. Reliab. Eng. Int.* **2016**, *32*, 2987–2994. [CrossRef]
23. Riaz, M. A sensitive non-parametric EWMA control chart. *J. Chin. Inst. Eng.* **2015**, *38*, 208–219. [CrossRef]
24. Riaz, M.; Abbasi, S.A. Nonparametric double EWMA control chart for process monitoring. *Rev. Colomb. Estadística* **2016**, *39*, 167–184. [CrossRef]
25. Xue, L.; An, L.; Feng, S.; Liu, Y.; Wu, H.; Wang, Q. A nonparametric adaptive EWMA control chart for monitoring multivariate time-between-events-and-amplitude data. *Comput. Ind. Eng.* **2024**, 110250. [CrossRef]
26. Zhou, Q.; Zou, C.; Wang, Z.; Jiang, W. Likelihood-based EWMA charts for monitoring Poisson count data with time-varying sample sizes. *J. Am. Stat. Assoc.* **2012**, *107*, 1049–1062. [CrossRef]
27. Qi, D.; Wang, Z.; Zi, X.; Li, Z. Phase II monitoring of generalized linear profiles using weighted likelihood ratio charts. *Comput. Ind. Eng.* **2016**, *94*, 178–187. [CrossRef]
28. Qi, D.; Li, Z.; Zi, X.; Wang, Z. Weighted likelihood ratio chart for statistical monitoring of queueing systems. *Qual. Technol. Quant. Manag.* **2017**, *14*, 19–30. [CrossRef]
29. Zhang, C.; Tsung, F.; Xiang, D. Monitoring censored lifetime data with a weighted-likelihood scheme. *Nav. Res. Logist. (NRL)* **2016**, *63*, 631–646. [CrossRef]
30. Yu, M.; Wu, C.; Wang, Z.; Tsung, F. A robust CUSUM scheme with a weighted likelihood ratio to monitor an overdispersed counting process. *Comput. Ind. Eng.* **2018**, *126*, 165–174. [CrossRef]
31. Yao, C.; Li, Z.; He, C.; Zhang, J. A Phase II control chart based on the weighted likelihood ratio test for monitoring polynomial profiles. *J. Stat. Comput. Simul.* **2020**, *90*, 676–698. [CrossRef]

32. Song, Z.; Liu, Y.; Li, Z.; Zhang, J. A weighted likelihood ratio test-based chart for monitoring process mean and variability. *J. Stat. Comput. Simul.* **2018**, *88*, 1415–1436. [CrossRef]
33. Xie, M.; Goh, T.N.; Tang, X.Y. Data transformation for geometrically distributed quality characteristics. *Qual. Reliab. Eng. Int.* **2000**, *16*, 9–15. [CrossRef]
34. Reynolds, M.R., Jr.; Lou, J. An Evaluation of a GLR Control Chart for Monitoring the Process Mean. *J. Qual. Technol.* **2010**, *42*, 287–310. [CrossRef]

Disclaimer/Publisher's Note: The statements, opinions and data contained in all publications are solely those of the individual author(s) and contributor(s) and not of MDPI and/or the editor(s). MDPI and/or the editor(s) disclaim responsibility for any injury to people or property resulting from any ideas, methods, instructions or products referred to in the content.